Scientia Iranica C (2022) 29(3), 1308–1318

Sharif University of Technology
Scientia Iranica
Transactions C: Chemistry and Chemical Engineering
http://scientiairanica.sharif.edu

Simultaneous spectrofluorometric analysis of caffeic and ellagic acids through inclusion complex formation with γ-cyclodextrin

M. Abedi*, M. Mikani, and R. Rahmanian

Department of Chemical Technologies, Iranian Research Organization for Science and Technology (IROST), Tehran, P.O. Box 33535-111, Iran.

Received 8 August 2020; received in revised form 4 May 2021; accepted 22 November 2021

KEYWORDS
Caffeic acid;
Ellagic acid;
Second-order advantage;
γ-cyclodextrin;
BLLS/RBL;
Fruit juice.

Abstract. The extraordinary sensitivity of fluorescence spectroscopy has brought it to chemists' attention. Spectra recording at several interval times while the reaction is preceded, or at different complexing factor concentrations, is one case of policies by which data (second-order) can be created using the spectrofluorometric technique. In the current case, a mixed fluorescence spectrum of two Caffeic Acid (CA) and Ellagic Acid (EA) target analytes was documented as a γ-cyclodextrin (γ-CD) function (as an inclusion complexing factor) to produce data (second-order). At this point, Bilinear Least Squares/Residual Bilinearization (BLLS/RBL), as a second-order calibration technique, due to its benefits of accuracy, rapidity, simplicity, suitable concentration, and spectral resolution estimation even in the presence of the unknown interference (second-order advantage) was exploited for trilinear data deconvolution to obtain fluorescence spectra and concentration profiles of the EA and CA as a function of γ-CD concentrations. A set of calibrations comprising 10 reference samples was employed to build the BLLS/RBL procedure. By a test set including 6 samples, the predictive ability of the technique was validated. The suggested model was effectively exploited to quantify CA and EA content in four fruit juice samples.

1. Introduction

Upon the achievement of second-order calibration through matrices, a novel and revolutionary benefit is attained named "second-order advantage" [1]. This calibration variant is also called 'three-way' since sample set matrices can be joined into a 3-way data array. The order recognizes the instrumental mode number for one sample and also, the ways that the modes are quantified for a sample set. The second-order advantage indicates that although the signal of interferents in unknown samples cannot only be identified, it is exactly modeled [2–5]. The contribution of interferents can be isolated from analyte, and consequently the analyte approximation may carefully progress without necessity for experimental separation of the interferences [3–6].

Multi-way calibration expresses the potential of realizing the analytical chemistry dream given that:

(i) Selectivity and sensitivity are enhanced as the number of instrumental modes increases;

(ii) Only small, pure-analyte calibration sets are demanded instead of huge calibration sets com-

*. *Corresponding author. Tel.: +98 21 65276637*
Fax: +98 21 56276265
E-mail address: mabedi50@yahoo.com (M. Abedi)

doi: 10.24200/sci.2021.56575.4795

prising all conceivable interferents (as wanted by first-order multivariate calibration);

(iii) The second-order advantage can be attained; simply put, analytes are quantitated in the presence of uncalibrated interferents;

(iv) A full chromatographic resolution is not essential, separation investigations are shorter and simpler, and the number of instrumental modes increases;

(v) Sample clean-up stages may no longer be required [2–6].

In the current investigation, the authors showcase a reliable, accurate, cheap, and robust approach to produce second-order data based on created complexes (analytes...γ-CD). The environment dielectric possessions are identified and they affect spectral and molecular characteristics including the fluorescence position and the intensity of the peak in the spectra. Therefore, the molecule possessions entrenched in a cavity of CD can be projected to vary from those detected in water. In the existing scheme, fluorescence fluctuations resulting from the differences in the γ-CD concentrations present the γ-CD spectra (fluorescence)-concentration matrix data, and binding these data matrices for a sample set generates a 3-way array [7–9].

Phenolic acids are elaborated in numerous physiological events such as enzyme activity, photosynthesis, protein synthesis, and cytoskeleton assembly [10,11]. Ellagic acid (EA, 4,4,5,5,6,6-hexahydroxidifenic acid 2,6,2,6-dilactone) and caffeic acid (CA, 3,4-dihydroxycinnamic acid) are phenolic acid examples that are exploited as additives in pharmaceutical and cosmetics manufacturing due to their many use cases like antioxidant, antibacterial, and anticancer [10–15]. Many analytical methodologies have been employed for phenolic acid determination, comprising gas chromatography-mass spectrometry [14,15], capillary electrophoresis techniques [16], micellar electrokinetic chromatography [17], and HPLC [18]. The described performances not only comprise sophisticated equipment but also are time-consuming and challenging to apply to a multifaceted sample analysis [19].

The purpose of the current investigation is to propose a robust fluorescence technique based on complexes of γ-CD as an advanced performance to fabricate a 3-way data set for simultaneous determination of multicomponent in the presence of CA and EA. Determination of CA and EA in nutrition examples (fruit juice samples) is a significant analytical mission. Furthermore, to deliver the maximum discrimination between two analytes spectra, numerous experimentation factors were deliberated and improved. The concentration deconvolution of γ-CD-resolved fluorescence spectra is done using BLLS/RBL. In conclusion, figures of merit, predictive ability, and accuracy are projected to exhibit its prospective as a substitute for CA and EA determination, even in the presence of unexpected or unmodeled interferents and without sample pretreatments [20–22].

2. Experimental

The exploited components were of analytical reagent grade and acquired from Aldrich (Chemical Co., Milwaukee, WI, USA) or Merck (Darmstadt, Germany). Distilled water was exploited through the investigations. Marketable fruit juices were achieved from a superstore. The γ-CD was recrystallized twice from double-distilled water before the procedure.

The stock individual solutions (100 mg L^{-1}) of CA and EA were organized with an ethanol-water solution of 80% as a solvent. The CA and EA calibration mixture solutions were arranged by the stock calibration solutions with an 80% ethanol-water solution as a diluter. For construction of inclusion complexes under optimal situations, proper amounts of CA and EA standard solutions were placed in a 10.0 mL volumetric flask. Then, the suitable quantity of γ-CD (in range $2\times10^{-3}-1\times10^{-2}$ g L^{-1}) solution was mixed and pH = 4 was adjusted. Each solution was sheltered from light by aluminum foil and was preserved at 4°C.

By using a Cary Eclipse Xenon lamp 80 Hz model spectrofluorometer organized exploiting a thermostated cell compartment, the fluorescence spectra were achieved. Quantities were achieved in a 1 cm quartz cell (25 ± 0.1°C). The emission fluorescence data of samples were taken in the range of 420 to 470 nm with 1 nm increment in the excitation wavelength of 285 nm against the blank by spectrofluorometer with respectable reproducibility. The spectral area, 420–470 nm, was chosen because of maximum spectral information about the component mixture of interest. Furthermore, at this point, the data were managed by exploiting chemometric investigation based on the second-order algorithms employing Bilinear Least Squares/Residual Bilinearization (BLLS/RBL) in conjunction with MVC2 program, which is a MATLAB graphical interface toolbox for second-order multivariate calibration [23]. The pH of solution was deliberated via pH meter (Metrohm, model 692, Herisau, Switzerland) systematized with a glass electrode. A 37-kHz ultrasonic water bath (Elmasonic E 30H, 240 W, Elma, Singen, Germany) was employed for supporting the inclusion complex formation.

The separation between CA and EA was accomplished in a Waters 2690 HPLC system equipped with a Waters AF online degasser and linked to a Waters model 996 photodiode array detector. Instrument control and data analysis were done exploiting

Millennium 3.20 software. Separation of CA and EA was attained on a reverse-phase waters symmetry C-18 column (250 mm × 4.6 mm) (Millipore, Milford, MA) at 30°C. Gradient solvent comprising methanol-double distilled water was employed at a flow rate of 1 mL min^{-1}. Both standard and real samples injection volume was 20 μL. Retention times were exploited for the desired compounds documentation and peak zones determined at various concentrations were employed to plot calibration lines for each analyte. Before injection into a column, all solutions were cleaned upon applying 0.45 μm filters to omit insoluble resources.

3. Theoretical background

3.1. BLLS/RBL

The initial stage is the vectorization of each data matrix of calibration set $\mathbf{X}$ (each of size $J \times K$) and the I_c calibration samples are grouped in a matrix $\mathbf{V}_x$ of dimension $(JK \times I_c)$:

$$\mathbf{V}_x = [vec(\mathbf{X}_1)|vec(\mathbf{X}_2)|\cdots|vec(\mathbf{X}_{Ic})], \quad (1)$$

where "*vec*" is the procedure of unfolding the matrix into the vector.

The subsequent step uses direct least squares [20] to gain information on the pure-analyte matrices at the unit concentration ($\mathbf{V}_S$) in a technique analogous to first-order classical least squares:

$$\mathbf{V}_S = \mathbf{V}_x \mathbf{Y}^+, \quad (2)$$

where $\mathbf{Y}$ is an $I \times N_C$ matrix of the reference concentrations and N_C the number of calibrated analytes. $\mathbf{V}_S(JK \times N_C)$ contains the required $\mathbf{S}_n$ matrices in the vectorized form:

$$\mathbf{V}_S = [vec(\mathbf{S}_1)|vec(\mathbf{S}_2)|\cdots|vec(\mathbf{S}_{Nc})]. \quad (3)$$

To get the spectral profiles from the estimated matrix, Singular Value Decomposition (SVD) is employed at each estimated matrix ($\mathbf{S}_n$) obtained after appropriate reshaping of the unfolded vec ($\mathbf{S}_n$) [20]:

$$(\mathbf{b}_n,\ g_n,\ \mathbf{c}_n) = SVD(\mathbf{S}_n), \quad (4)$$

where g_n is the first singular value; $\mathbf{b}_n$ and $\mathbf{c}_n$ are $J \times 1$ and $K \times 1$, the first left and right singular vectors of $\mathbf{S}_n$, respectively.

The concentration in an unknown sample (whose matrix data are $\mathbf{X}_u$) can be estimated, provided that no interference occurs through direct least squares procedure [20]:

$$\mathbf{Y}_u = \mathbf{S}_{cal}^+ vec(\mathbf{X}_u), \quad (5)$$

where $\mathbf{Y}_u$ is an $N_C \times 1$ vector of the estimated concentration of the N_C analytes in the sample and $\mathbf{S}_{cal}$ is a calibration $JK \times N_C$ matrix given by:

$$S_{cal} = [g_1(\mathbf{c}_1 \otimes \mathbf{b}_1)|g_2(\mathbf{c}_2 \otimes \mathbf{b}_2)|\cdots|g_{Nc}(\mathbf{c}_{Nc} \otimes \mathbf{b}_{Nc})|, \quad (6)$$

where $\otimes$ indicates the Kronecker product.

If there are uncalibrated compounds in a test sample, residual bilinearization (RBL) should be coupled with BLLS [2]. The RBL technique is an iterative procedure that analyzes the matrix of residuals of the prediction least squares fit to approximate the interference profiles. Furthermore, this process serves to progress the loadings and to correctly approximate the analyte concentrations.

In this effort, two figures of merit namely sensitivity and Limit Of Detection (LOD) are estimated based on second-order calibration models. The sensitivity of (SEN) can be computed through a general expression [2]:

$$SEN = z_n\{[(\mathbf{B}^T\mathbf{B})(\mathbf{C}^T\mathbf{C})]^{-1}\}^{-1/2}. \quad (7)$$

For the BLLS, z_n is the first singular value gained by the SVD decomposition and $\mathbf{B}$ and $\mathbf{C}$ are the fluorescence and concentration profiles, respectively, for the calibrated analytes obtained by BLLS.

The LOD can be estimated using the expression [4]:

$$LOD = 3.3SD(0), \quad (8)$$

where $SD(0)$ is the estimated standard error in the predicted concentration for samples of zero or low analyte concentration [22]. Given that various samples have a different value of $SD(0)$, an average value over a calibration set of LOD is reported.

The Root Mean Squares Error of the Calibration (RMSEC) and Prediction samples (RMSEP) are two statistical parameters that express the accuracy of the model [22]. They report the closeness of agreement between the reference value and the value found by the model. These parameters can be written as follows:

$$RMSEC = \sqrt{\frac{\sum_{i=1}^{I}(c_i - \hat{c}_i)^2}{I-1}}, \quad (9)$$

where c_i and $\hat{c}_i$ are the real and predicted concentrations of the given analyte in the ith calibration sample, respectively.

$$RMSEC = \sqrt{\frac{\sum_{h=1}^{H}(c_h - \hat{c}_h)^2}{H-1}}, \quad (10)$$

where c_h and $\hat{c}_h$ are the real and predicted concentrations of the given analyte in the h_{th} test sample set, respectively. H is the total number of samples in the test set.

4. Results and discussion

4.1. Analytical process

The CDs (cyclic oligosaccharides with D-glucose units) comprise a hydrophilic outer platform and a moderately hydrophobic inside cavity [8]. This peculiar structure characteristic allows CDs to build host-guest inclusion complexes with an extensive range of compounds via non-covalent forces such as van der Waals forces, hydrophobic interactions, and hydrogen bonds [8,9]. The dominant complex formation driving power is the enthalpy-rich water molecules release from the internal cavity [24,25]. Water molecules that are replaced by more hydrophobic guest molecules exist in the solution consequences in the inclusion complex construction between the host and the guest. The inclusion complexing factor gives the outcomes and the degree of variation between analytes spectra. α, β, and γ-CDs are considered as complexing mediators. Among the three CDs, the comparison was done under the finest circumstances. It was obtained that the differentiation grade between analytes spectra was very low when α, β-CDs were exploited as complexing factors. Accordingly, γ-CD was selected.

Furthermore, in this case, for a mixture of CA and EA, bilinear data is attained by documenting fluorescence spectra at various concentrations of γ-CD, given the formation of the inclusion complex. Then, the data of fluorescence jointed the second-order calibration algorithms for simultaneous CA and EA analysis in complex real samples. To accomplish the formation of maximum inclusion γ-CD complexes with CA and EA targets, initially, numerous investigational factors were considered and improved. Besides, under optimum circumstances, BLLS/RBL algorithms were exploited for CA and EA simultaneous determination.

4.2. pH effect on formation of inclusion complexes

The hydrophobic cavity of CDs allows for exceptional capacity to snare a guest molecule inside its cavity. Nevertheless, the fabricated complex stability is pH dependent [24,25]. Owing to the existence of acidic group in the CA and EA structure, the corresponding species forms are adjustable with respect to pH values (more details in supplementary information). CA and EA exist as neutral molecules in acidic media because of ionization prevention. In a basic situation, this condition is overturned. As γ-CD cavity is hydrophobic, inclusion complexes are positively made with CA and EA neutral forms. The outcomes of γ-CD including CA (1 μg mL^{-1}) and EA (1 μg mL^{-1}) in 0.006 M γ-CD at different pH values (attuned by NaOH and HCl) are exposed, as given in Figure 1. The consequences illustrate that extreme fluorescence intensities are performed at pH 4.0 and reduced with the growing pH values. Based on Figure 1, pH 4.0 was selected for additional experiments.

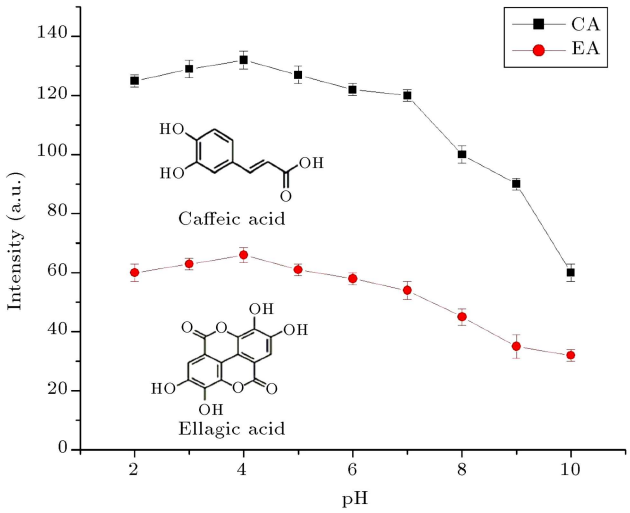

Figure 1. The fluorescence intensities of CA (1 μg mL^{-1}) and EA (1 μg mL^{-1}) in 0.006 M γ-CD concentration at different pH values.

4.3. Ionic strength effect on γ-CD including CA and EA

Employing a series of experiments in the presence of $NaNO_3$ allows investigating whether anion or cation has a powerful influence on the complex construction. If so, the ionic strength is operative. The concentration of $NaNO_3$ varies from 0.01 to 0.1 M. The consequences show a slight fluctuation in fluorescence once the $NaNO_3$ concentration varies (Figure 2). The ionic strength has a minor influence on the inclusion of target phenolic acids in γ-CD. Subsequently, no salt was added to later surveys. In addition, the temperature effects and sonication time were added

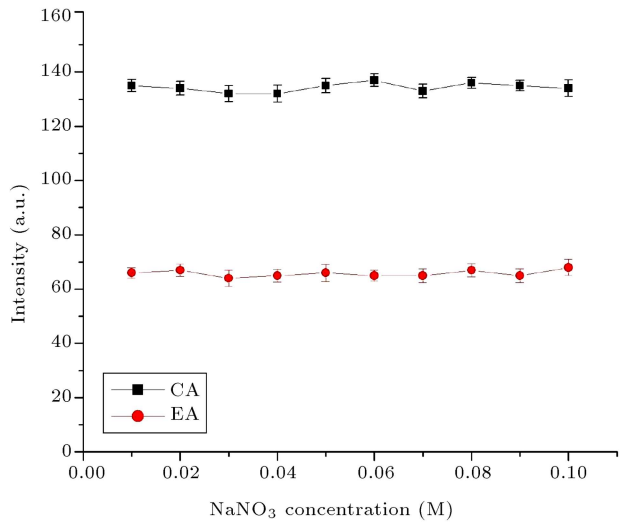

Figure 2. $NaNO_3$ salt concentration effect on 0.006 M γ-CD including CA (1 μg mL^{-1}) and EA (1 μg mL^{-1}).

Table 1. "Calibration samples" for prediction by BLLS/RBL method.

Samples	Caffeic acid (μg mL^{-1})		Ellagic acid (μg mL^{-1})	
	Real concentration	BLLS/RBL[a] result	Real concentration	BLLS/RBL result
1	3.00	3.00 (100.00) [b]	3.00	3.10 (103.30)
2	4.00	4.10 (102.50)	2.00	1.90 (95.00)
3	0.00	0.00 (–)	6.00	5.90 (98.30)
4	6.00	5.90 (98.3)	1.00	1.00 (100.00)
5	1.00	1.00 (100.0)	7.00	7.10 (101.40)
6	2.00	2.00 (100.0)	4.00	4.00 (100.00)
7	0.00	0.00 (–)	8.00	8.00 (100.00)
8	5.00	5.10 (102.0)	0.00	0.00 (–)
9	7.00	7.10 (101.4)	0.00	0.00 (–)
10	2.00	2.10 (105.0)	5.00	4.90 (98.00)
RMSEC (μg mL^{-1})	–	0.07	–	0.07
Mean recovery	–	101.10	–	99.50
Sensitivity (a.u. mL μg^{-1})	–	2e+002	–	1.1e±002
Selectivity	–	0.13	–	0.13
LOD ((μg mL^{-1}))	–	1.2e–006	–	3.3e–007
γ (analytical sensitivity, mL μg $^{-1}$)	–	1.5e±015	–	1.1e±016

[a] BLLS/RBL (2 analytes + 0 interferences); [b] Recovery in parenthesis.

to the supplementary information. In addition, in the supplementary information, the impacts of pH, ionic strength, and temperature on CA and EA fluorescence intensity were investigated using Response Surface Methodology (RSM).

4.4. Second-order multivariate calibration technique

4.4.1. Calibration and validation sample sets

To exhibit the linearity between fluorescence data and concentrations of analyte and to obtain each analyte linear range, a calibration plot was generated for both phenolic acids. The standard solution fluorescence data were achieved through the following steps: addition of γ-CD and changing of pH to 4.0. A calibration curve was designed with numerous points for each analyte as fluorescence in the range of 420–470 nm with 1 nm increment in excitation wavelengths of 285 nm against the blank versus sample concentrations. Through linear regression analysis, the plot was assessed. With squared correlation coefficients of 0.9996 and 0.9997, the linear range was detected from 0–7 to 0–8 μg mL^{-1} for CA and EA, individually.

After improving the inclusive circumstances, second-order multivariate calibration performances were employed to examine the CA and EA spectra for their simultaneous measurement. The primary stage is to plan and generate a calibration matrix (samples) $\times$ fluorescence $\times$ concentration of γ-CD), which is exploited for model training. Randomly, ten binary standard solutions were designated. The analytes concentrations were between 0–7 and 0–8 μg mL^{-1} for CA and EA, individually. The configurations of calibration mixtures are offered (Table 1). Randomly, the fabricated model was authenticated with 6 synthetic binary mixtures preferred (Table 2). The applicability of the model has also been studied for simultaneous CA and EA analysis in real samples.

4.4.2. Analytes spectral performance accompanied with data pretreatment

Figure 3 shows the normalized profiles of pure CA and EA recorded under optimum circumstances. The spectra display an extraordinary degree of overlap between CA and EA fluorescence peaks. Such an overlapping degree obstructs these analytes analysis in their mixture by the traditional univariate technique. To overcome this obstacle, a separation done through a mathematical process can be employed based on chemometrics techniques. To this end, second-order data such as the concentration of γ-CD-resolved fluorescence data matrices were reached and treated with BLLS/RBL, attaining the second-order advantage.

For the data with no planned pre-processing, in the present case, the 3-way data in the form of samples $\times$ fluorescence $\times$ concentration of γ-CD were gathered into 3 data cubes called calibration set (size $10 \times 51 \times 5$ ($I \times J \times K$)), validation set with the dimension of $6 \times 51 \times 5$ ($I \times J \times K$), and real samples of size $4 \times 51 \times 5$($I \times J \times K$) making 2550, 1530, 1020 data points for

Table 2. "Calibration samples" for prediction by BLLS/RBL method.

Samples no. (type of interference)	Caffeic acid (μg mL^{-1})		Ellagic acid (μg mL^{-1})	
	Real concentration	BLLS/RBL[a] Result	Real concentration	BLLS/RBL Result
1 (1 μg mL^{-1} vanillic acid)	5.50	5.40 (98.10) [b]	0.00	0.00 (–)
2 (1 μg mL^{-1} ascorbic acid)	0.00	0.00 (–)	4.50	4.40 (97.00)
3 (1 μg mL^{-1} gallic acid)	4.50	4.50 (100.00)	1.50	1.50 (100.00)
4 (1 μg mL^{-1} coumaric acid)	1.50	1.60 (106.60)	6.00	5.90 (98.30)
5 (1 μg mL^{-1} ferulic acid)	3.00	2.90 (96.60)	2.50	2.40 (96.00)
6 (1 μg mL^{-1} p-hydroxy benzoic acid)	2.50	2.50 (100.00)	5.00	5.10 (102.00)
RMSEP (μg mL^{-1})	–	0.07	–	0.08
Mean recovery	–	100.20	–	98.60

[a] BLLS/RBL (2 analytes + 0 interferences); [b] Recovery in parenthesis.

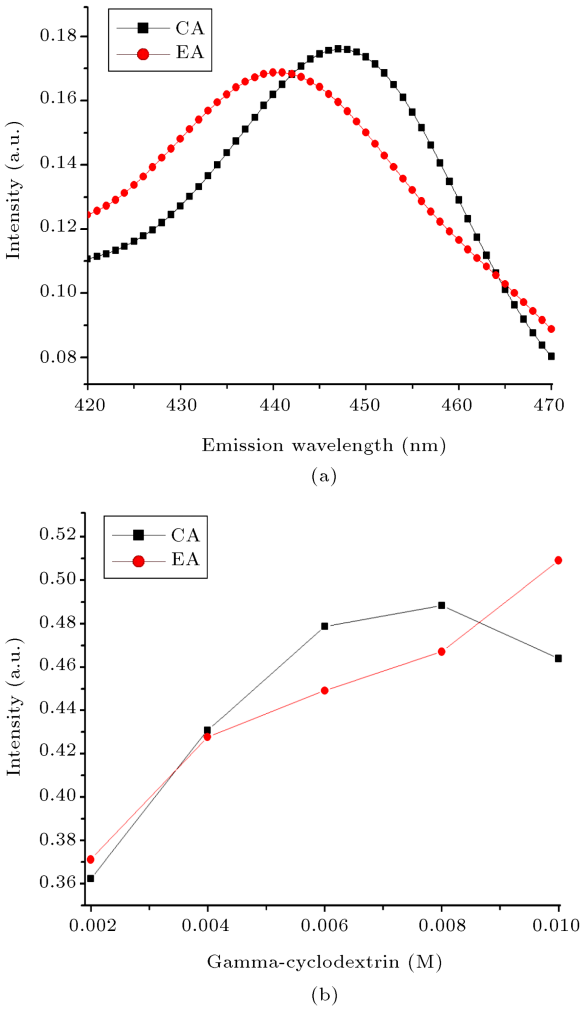

Figure 3. The normalized profiles of pure CA and EA, recorded under the optimum conditions: (a) Emission profile and (b) normalized γ-CD concentration profile.

each system. The present investigation displayed the fluorescence of EA and CA variations upon variation in the concentration of γ-CD. Second-order multivariate calibration employing BLLS/RBL was done using the MVC2 program. Before running MVC2, the spectral data were kept in a particular setup, which is well-matched with MVC2.

4.4.3. Prediction of CA and EA in the calibration set

Because of inadequate space, 3 data sets in the calibration set (Table 1) are as follows: 1, 7, and 9 are shown in Figure 4(a), (b), and (c). At first, the 3-way calibration data set was vectorized and unfolded in the sample direction to a size 10×255 matrix and BLLS/RBL was employed to model the data. The analyst's concentrations were identified and each analyte sensitivity vector was measured according to Eq. (2). By matricizing each sensitivity vector and applying SVD to it, each analyte pure profile was acquired. The calibrated analytes number and predictable interferences in BLLS/RBL modeling were set to 2 and 0, respectively. The interference number was supposed to be 0 because binary calibration mixtures were free from any interferences. After the model development, it can be exploited to estimate analytes concentrations in calibration, test, or any unknown samples consistently in the presence of interfering species. All figures of merit for the projected methods are projected in Table 1 where the net-analyte signal concept was employed [4]. In Table 1, RMSEC was considered as an indicator of the model accuracy. The calculated RMSEC values for the calibration set were 0.07 and 0.07 μg mL^{-1} for CA and EA, respectively. Low RMSEC values for the calibration set illustrated that the predictive ability of the BLLS/RBL model was appropriate. Sensitivity rates were computed as $2e^{+002}$ and $1.1e^{+002}$ a.u. mL μg^{-1} for CA and EA, respectively. Thus, it can be comprehended based on the consequences that the present model is very sensitive to the simultaneous quantification of CA and EA. In addition, from the selectivity result, it can be perceived that the current model is very selective for determining

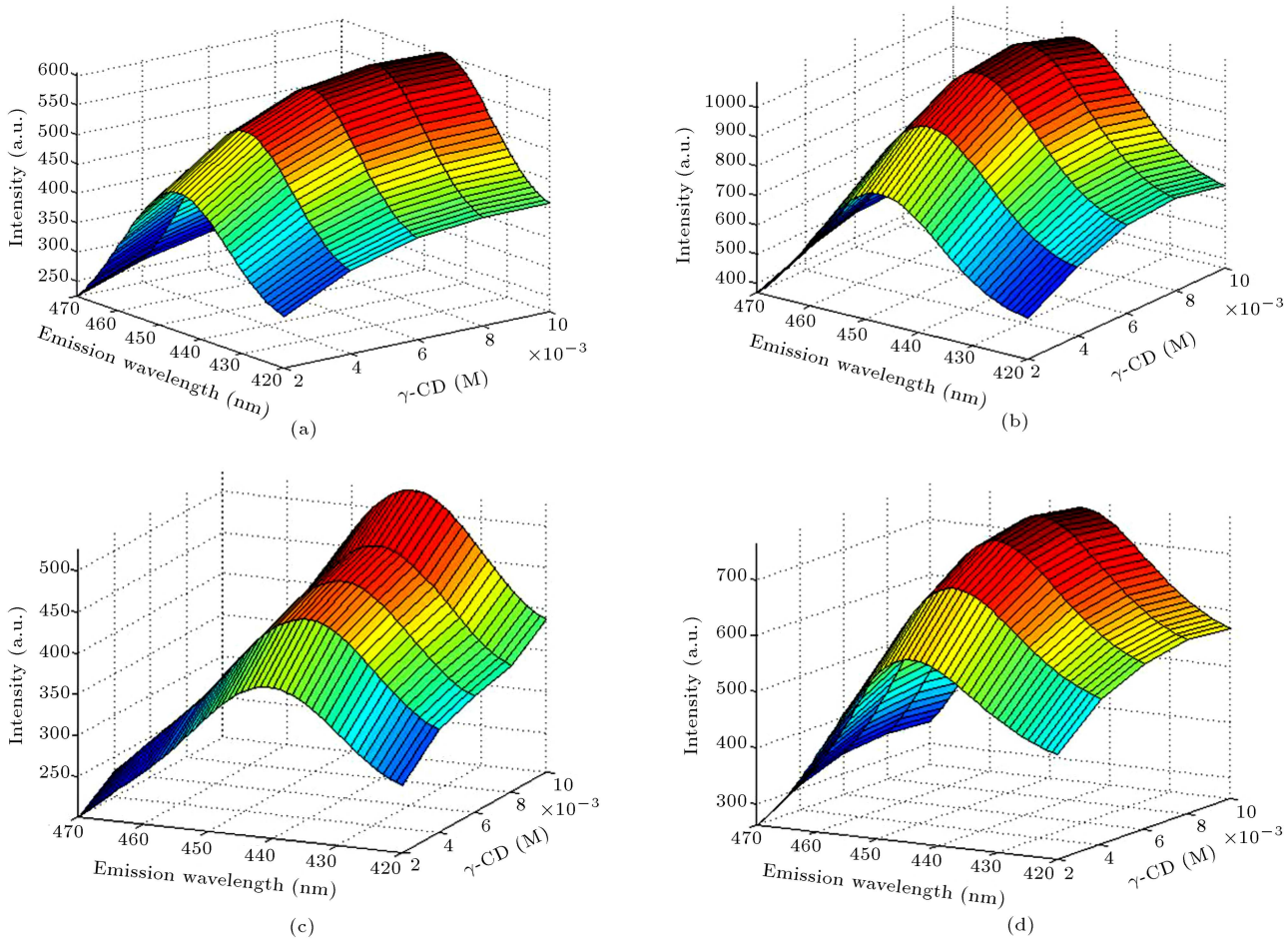

Figure 4. Calibration sample graphs: (a) Calibration 1, (b) calibration 7, (c) calibration 9, and (d) pomegranate juice 1.

CA and EA simultaneously. As implied earlier, a very noble fitting was achieved for both components. This fact reflects the high calibration power of the model.

4.4.4. Prediction in validation samples

The validation set was employed to survey the capability of the exploited procedure to determine CA and EA in the presence of interferences such as vanillic acid, ascorbic acid, gallic acid, coumaric acid, ferulic acid, and *p*-hydroxybenzoic acid (Table 2). The interference number of components was considered as 1 in samples in BLLS/RBL method. The outcomes of 6 validation samples are presented in Table 2 and Figure 5. Current technique can be used to predict the analytes concentration in mixtures. The RMSEP was deliberated as statistical factors to display the accuracy of consequences, as shown in Table 2. The calculated RMSEP values for the validation set were 0.07 and 0.08 μg mL^{-1} for CA and EA, respectively. The RMSEP results represent excellent values.

4.4.5. Prediction in real samples

The fruit juice samples were kept at 4°C before usage. Each of fruit juice samples (5 mL) was centrifuged for 20 min at 3000 rpm. Through a 0.45 μm pore size membrane filter, the supernatant was cleaned and diluted to 50 mL. All of these real samples were clear and no sediments or suspensions were identified. Lastly, accurate volume of each organized real sample (10 mL) was investigated under the suggested process, and the precise CA and EA concentrations in the original samples were then measured with the aid of BLLS/RBL as a 2-order calibration technique. Figure 4(d) displays the 3D plot of pomegranate juice.

Our main goal in the present survey was the simultaneous quantification of CA and EA with intensely overlapped spectra in real samples which cover uncalibrated interferences. Now, the BLLS/RBL performance capability to study real samples was studied. Real samples containing 4 types were deliberated, and to check the applied method accuracy, the concentrations of the known analytes were spiked in certain samples, as described in Table 3, and the analyte recovery were considered.

By exploiting BLLS/RBL in the data analysis, the interference numbers for real samples were set as 1 and the outcomes were assumed, as given in Table 3. Perfect recoveries for all the spiked samples

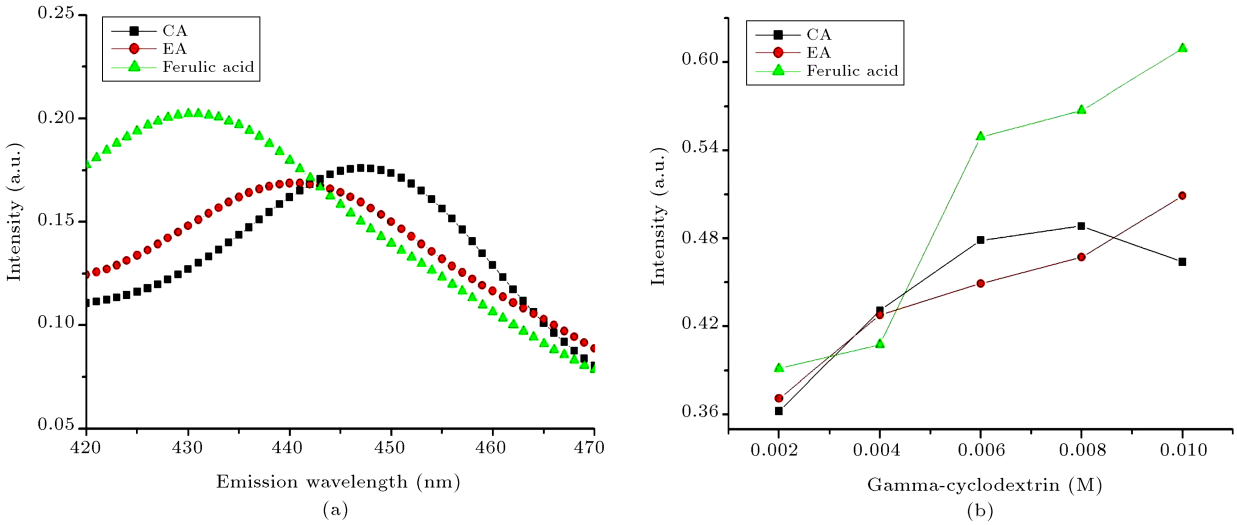

Figure 5. The resolved profiles from BLLS/RBL for the validation sample number 5.

Table 3. "Real samples" for prediction by BLLS/RBL and HPLC methods.

Samples	BLLS/RBL[a]						HPLC	
	Spiked (μg mL^{-1})		Predicted (μg mL^{-1})		Recovery%		Predicted (μg mL^{-1})	
	Caffeic acid	Ellagic acid	Caffeic acid	Ellagic acid	Caffeic acid	Ellagic acid	Caffeic acid	Ellagic acid
Purple grape juice								
NO. 1	–	–	1.00	2.00	–	–	0.90	2.00
NO. 2	2.00	–	2.95	2.00	97.00	–	3.00	2.01
NO. 3	2.00	2.00	3.10	3.98	105.00	99.00	3.00	3.98
Strawberries juice								
NO. 1	–	–	3.02	2.00	–	–	3.00	1.98
NO. 2	1.00	–	4.12	2.00	110.00	–	4.10	1.99
NO. 3	1.00	2.00	3.98	4.01	96.00	100.00	3.99	4.00
NO. 4	2.00	1.00	5.05	2.99	101.50	99.00	4.99	3.02
Apple juice								
NO. 1	–	–	5.00	2.00	–	–	4.99	1.99
NO. 2	1.00	1.00	6.01	3.05	101.00	105.00	5.98	2.99
NO. 3	1.00	–	5.98	2.03	98.00	–	5.97	2.01
NO. 4	–	1.00	5.00	2.93	–	93.00	4.98	2.99
Pomegranate juice								
NO. 1	–	–	1.50	4.50	–	–	1.50	4.50
NO. 2	2.00	1.00	3.40	5.55	95.00	105.00	3.50	5.48
NO. 3	1.00	1.00	2.50	5.49	100.00	99.00	2.49	5.48

[a] BLLS/RBL (2 analytes + 1 interferences).

were detected. The analytes recovery was considered according to Eq. (11):

$$\%Recovery = \frac{h_p - h_{real}}{h_{added}} \times 100, \tag{11}$$

where h_p is predicted concentration (sum of real concentration and added amount), h_{real} the real sample concentration without any added amount, and h_{added} the concentration amount which is added to real the concentration.

Figure 6 exhibits the achieved profiles for each analyte along with the interference profile. Considering the provided spectra presented in Figure 6, the high similarity between the attained analytes spectral

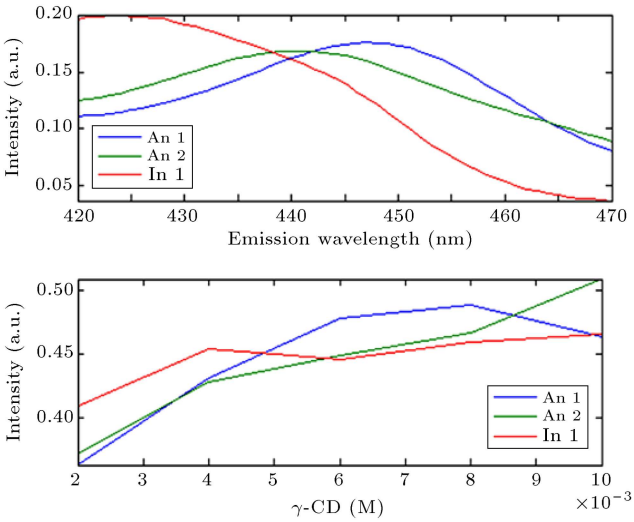

Figure 6. The resolved profiles from BLLS/RBL for the pomegranate juice (An1:CA, An2:EA).

profiles and their real profiles (Figure 3), regardless of the complexity of the studied matrix, demonstrated the reliability and accuracy of the proposed approach, which is a fully employed second-order advantage. Moreover, the data were investigated by PARAFAC whose consequences were compared with BLLS/RBL in the supplementary information.

4.4.6. Real samples HPLC analysis

To prove the capability of the current performance in samples to determine CA and EA phenolic acids simultaneously and to approximate the result of the sample matrix on the analytes recovery, the analysis of the fruit juice samples was conducted. The HPLC consequences acquired were compared with those achieved from BLLS/RBL. The predicted CA and EA concentrations are shown in Table 3 and the chromatograms are presented in Figure 7. The results show no substantial differences between the reference method (HPLC) and the approach designated in the current case. The exceptional combination of original analyses and outcomes of high-resolution measurable procedures with a great prospective for upcoming surveys would be exploited [26–32].

5. Conclusion

A robust technique for the simultaneous quantification of CA and EA in fruit juice examples from fluorescence spectra in 80% ethanol-water mixed solvents using BLLS/RBL was established. Until now, numerous approaches have been exploited for the fabrication of second-order data. This investigation described the utilization of γ-CD complexes as an original attitude to generate 3-way data, jointed with 2-order calibration based on the BLLS/RBL algorithm, employing the second-order advantage. This combination can be

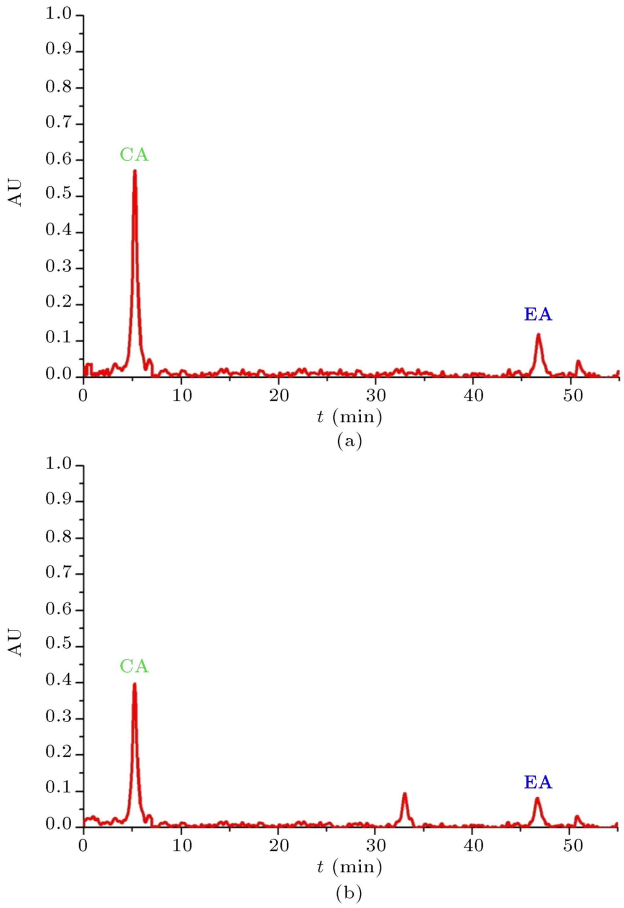

Figure 7. Pure chromatogram for (a) 3 μg mL^{-1} solutions of EA and CA and (b) for sample of apple juice.

effectively implemented for multicomponent quantification in the presence of unexpected sample matrix components. Second-order calibration approaches could expect exact concentrations and a sensible resolution of spectral profiles for the analytes of interest from any uncalibrated interferences on account of "second-order advantage". The projected technique was effectively exploited to measure CA and EA simultaneously in the spiked fruit juice samples with high recoveries and low prediction errors. It was also employed to analyze real fruit juice samples with the results close to those obtained by the HPLC technique. Although only applied to quantify simultaneously CA and EA in fruit juice samples as designated in this paper, the advanced second-order data species may be normally appropriate to measure simultaneously other analytes in foodstuffs using second-order calibration algorithms or other chemometric performances.

Acknowledgment

The authors acknowledge the Iranian Research Organization for Science and Technology (IROST) for financially supporting this study.

Supplementary data is available at

file:///C:/Users/SHAMILA/AppData/Local/Temp/Supplementary

References

1. Kiers, H.A.L. and Smilde, A.K. "Some theoretical results on second-order calibration methods for data with and without rank overlap", *J. Chemom.*, **9**, pp. 179–195 (1995).
2. Sajjadi, S.M., Abdollahi, H., Rahmanian, R., et al. "Quantifying aflatoxins in peanuts using fluorescence spectroscopy coupled with multi-way methods: Resurrecting second-order advantage in excitation-emission matrices with rank overlap problem", *Spectrochim. Acta A.*, **156**, pp. 63–69 (2016).
3. Khani, R., Rahmanian, R., and Motlagh, N.V. "UV-visible spectrometry and multivariate calibration as a rapid and reliable tool for simultaneous quantification of ternary mixture of phenolic acids in fruit juice samples", *Food Anal. Method*, **9**, pp. 1112–1119 (2016).
4. Asadpour-Zeynali, K., Sajjadi, S.M., Taherzadeh, F., et al. "Analysis of variation matrix array by bilinear least squares-residual bilinearization (BLLS-RBL) for resolving and quantifying of foodstuff dyes in a candy sample", *Spectrochim. Acta A.*, **123**, pp. 273–281 (2014).
5. Khani, R., Ghasemi, J.B., Shemirani, F., et al. "Application of bilinear least squares/residual bilinearization in bulk liquid membrane system for simultaneous multicomponent quantification of two synthetic dyes", *Chemom. Intell. Lab. Syst.*, **144**, pp. 48–55 (2015).
6. Azzouz, T., and Tauler, R. "Application of multivariate curve resolution alternating least squares (MCR-ALS) to the quantitative analysis of pharmaceutical and agricultural samples", *Talanta*, **74**, pp. 1201–1210 (2008).
7. Loftsson, T., and Brewster, M.E. "Pharmaceutical applications of cyclodextrins. Drug solubilization and stabilization", *J. Pharm. Sci.*, **85**, pp. 1017–1025 (1996).
8. Del Valle, E.M.M. "Cyclodextrins and their uses: A review", *Process Biochem.*, **39**, pp. 1033–1046 (2004).
9. Szente, L., Szejtli, J., and Kis, G.L. "Spontaneous opalescence of aqueous gamma-cyclodextrin solutions-complex-formation or self-aggregation", *J. Pharm. Sci.*, **87**, pp. 778–781 (1998).
10. Saldanha, E., Joseph, N., Kumar, A., et al. "Polyphenols in human health and disease", Chapter 31 - *Polyphenols in the Prevention of Acute Pancreatitis: Preclinical Observations*, **1**, pp. 427–433 (2014).
11. Shivashankara, A.R., Sunitha, V., Bhat, H.P., et al. "Bioactive food as dietary interventions for liver and gastrointestinal disease", *Chapter 47 - Phytochemicals are effective in the prevention of ethanol-induced hepatotoxicity: Preclinical Observations.*, **1**, pp. 743–758 (2013).
12. Hao, D.C., Gu, X.J., and Xiao, P.G. "14 - Phytochemical and biological research of Salvia medicinal resources", *Medicinal Plants, Chemistry. Biology and Omics*, **1**, pp. 587–639 (2015).
13. Magnani, C., Isaac, V., Corrêa, M.A., et al. "Caffeic acid: A review of its potential use in medications and cosmetics", *Anal. Methods*, **6**, pp. 3203–3210 (2014).
14. Zadernowski, R., Czaplicki, S., and Naczk, M. "Phenolic acid profiles of mangosteen fruits (Garcinia mangostana)", *Food Chem.*, **112**, pp. 685–689 (2009).
15. Saraji, M., and Mousavinia, F. "Single-drop microextraction followed by in-syringe derivatization and gas chromatography-mass spectrometric detection for determination of organic acids in fruits and fruit juices", *J. Sep. Sci.*, **29**, pp. 1223–1229 (2006).
16. Helmja, K., Vaher, M., Puessa, T., et al. "Bioactive components of the hop strobilus: Comparison of different extraction methods by capillary electrophoretic and chromatographic methods", *J. Chromatogr. A.*, **1155**, pp. 222–229 (2007).
17. Huang, H.Y., Lien, W.C., and Chiu, C.W. "Comparison of microemulsion electrokinetic chromatography and micellar electrokinetic chromatography methods for the analysis of phenolic compounds", *J. Sep. Sci.*, **28**, pp. 973–981 (2005).
18. Klejdus, B., Vacek, J., Lojkova, L., et al. "Ultrahigh-pressure liquid chromatography of isoflavones and phenolic acids on different stationary phases", *J. Chromatogr. A.*, **1195**, pp. 52–59 (2008).
19. Makris, D.P., Kallithraka, S., and Mamalos, A. "Differentiation of young red wines based on cultivar and geographical origin with application of chemometrics of principal polyphenolic constituents", *Talanta*, **70**, pp. 1143–1152 (2006).
20. Linder, M., and Sundberg, R. "Precision of prediction in second-order calibration, with focus in bilinear regression method", *J. Chemom.*, **16**, pp. 12–27 (2002).
21. Damiani, P.C., Nepote, A.J., Bearzotti, M., et al. "A test field for the second-order advantage in bilinear least-squares and parallel factor analyses: fluorescence determination of ciprofloxacin in human urine", *Anal. Chem.*, **76**, pp. 2798–2806 (2004).
22. Leurgans, S., Ross, R., and Abel, R. "Decomposition for three-way arrays", *J. Matrix Anal. Appl.*, **14**, pp. 1064–1083 (1993).
23. Olivieri, A.C., Wu, H., and Yu, R. "MVC2: A MATLAB graphical interface toolbox for second-order multivariate calibration", *Chemom. Intell. Lab. Syst.*, **96**, pp. 246–251 (2009).
24. Baglole, K.N., Boland, P.G., and Wagner, B.D. "Fluorescence enhancement of curcumin upon inclusion into parent and modified cyclodextrins", *J. Photoch. Photobio. A.*, **73**, pp. 230–237 (2005).

25. Fini, P., Loseto, R., Catucci, L., et al. "Agostiano, study on the aggregation and electrochemical properties of Rose Bengal in aqueous solution of cyclodextrins", *Bioelectrochem.*, **70**, pp. 44–49 (2007).
26. Mikani, M., Talaei, S., Rahmanian, R., et al. "Sensitive electrochemical sensor for urea determination based on F-doped SnO_2 electrode modified with ZnO-Fe_3O_4 nanoparticles transducer: Application in biological fluids", *J. Electroanal. Chem.*, **840**, pp. 285–294 (2019).
27. Mikani, M., Rahmanian, R., Karimnia, M., et al. "Novel I-V disposable urea biosensor based on a dip-coated hierarchical magnetic nanocomposite (Fe_3O_4@SiO_2@NH_2) on FTO Layer", *J. Chin. Chem. Soc.*, **64**, pp. 1446–1459 (2017).
28. Mikani, M., Torabizadeh, H., and Rahmanian, R. "Magnetic soy protein isolate-bovine serum albumin nanoparticles preparation as a carrier for inulinase immobilization", *IET Nanobiotechnol.*, **12**, pp. 633–639 (2018).
29. Mikani, M., Torabizadeh, H., and Rahmanian, R. "Inulin hydrolysis by immobilized inulinase on functionalized magnetic nanoparticles using soy protein isolate and bovine serum albumin", *J. Chin. Chem. Soc.*, **65**, pp. 771–779 (2018).
30. Moharamzadeh, M.R., Salar Amoli, H., Rahmanian, R., et al. "Cu^{2+}-doped ITO as a novel efficient, transparent, and fast-response transducer for ammonia sensing", *J. Chin. Chem. Soc.*, **65**, pp. 735–742 (2018).
31. Mikani, M. and Rahmanian, R. "Sensitive biosensor based on urease/In_2O_5Sn nano-coated fluorinated SnO_2 for urea detection in blood serum", *J. Anal. Chem.*, **76**, pp. 981–992 (2021).
32. Hassan-Zadeh, B., Rahmanian, R., Salmani, M.H., et al. "Functionalization of synthesized nanoporous silica and its application in malachite green removal from contaminated water", *J. Environ. Health Sustain. Dev.*, **6**, pp. 1311–1320 (2021).

Biographies

Mohammad Abedi received his PhD in Analytical Chemistry from Isfahan University. His main areas of interests include green chemistry, food analysis, nanotechnology, and solar cells.

Mohaddeseh Mikani received her MSc in Food Industry from the Department of the Chemical Technology of Iranian Research Organization for Science and Technology (IROST). Her main areas of interests include nanotechnology, chemometrics, biotechnology, and food science.

Reza Rahmanian received his PhD in Chemistry from the Department of the Chemical Technology of Iranian Research Organization for Science and Technology (IROST). His main areas of interests include chemometrics, biosensors, thin layers and nanotechnology, and solar cells.